

Unusual sequence of phase transitions in MnAs: First-principles study

L. M. Sandratskii and E. Şaşıoğlu

Max-Planck Institut für Mikrostrukturphysik, D-06120 Halle, Germany

(Received 30 August 2006; revised manuscript received 7 November 2006; published 22 December 2006)

The frozen-magnon approach is employed to calculate the exchange parameters and critical temperatures of α and β MnAs. The data obtained are used to interpret the properties of the sequence of phase transitions in the material. It is found that the system, despite well-defined Mn moments, cannot be quantitatively described within the Heisenberg model. This conclusion is related to the properties of induced As moments. An unusual nonmonotonous dependence of the induced As moments on the net magnetization of the Mn sublattice is obtained. It is shown that such a behavior can be the reason for the canting of the Mn moments.

DOI: [10.1103/PhysRevB.74.214422](https://doi.org/10.1103/PhysRevB.74.214422)

PACS number(s): 75.50.Cc, 75.30.Et, 74.62.-c

I. INTRODUCTION

For many decades, manganese arsenide has attracted the attention of researchers. Despite many efforts, the nature of the unusual sequence of phase transformations in MnAs remains a matter of debate.^{1,2} Other important features of the system are the similarity of the magnetoresistance properties to the colossal magnetoresistance in Mn perovskites³ and a strong magnetocaloric effect useful for magnetic refrigeration.⁴ The unusual properties of the bulk system are preserved in the MnAs films.⁵⁻⁷ The interest to MnAs has been recently strongly enhanced by the possible applications of the material in spintronic devices. (See Ref. 2 for a recent overview on MnAs.)

The phase transitions in bulk MnAs take place at temperatures $T_1=313$ K and $T_2=399$ K.⁸ The transformation at T_1 (α -MnAs to β -MnAs) is of the first order. It includes simultaneous discontinuous change of both crystal lattice and magnetic state. The crystal lattice changes from hexagonal NiAs type to orthorhombic MnP type. The magnetic state below T_1 is ferromagnetic. The nature of the nonferromagnetic β phase remains the subject of discussions. The assumption that the system is in an ordered antiferromagnetic⁹ state is not supported by neutron-diffraction experiments,^{10,11} which did not detect any long-range magnetic order. On the other hand, the temperature dependence of the magnetic susceptibility deviates strongly from the Curie-Weiss law typical for the paramagnetic state of systems with well defined atomic moments.

The β - γ phase transformation at T_2 is of the second order. At this point the crystal lattice continuously returns back to the NiAs type. Above T_2 , the magnetic susceptibility follows the Curie-Weiss law demonstrating that the system is now in a conventional paramagnetic state.

Different interpretations of the nature of the first-order phase transition at T_1 and the character of the magnetic state between T_1 and T_2 have been proposed. Kittel¹² assumed that at T_1 the exchange interaction changes sign from ferromagnetic to antiferromagnetic. On the other hand, Goodenough and Kafalas¹³ suggested that the phase transition takes place between a high-spin state ($T < T_1$) and a low-spin state ($T > T_1$). Bean and Rodbell⁸ have shown within a framework of a phenomenological thermodynamic treatment that the first-order phase transformation ferromagnet-paramagnet is pos-

sible in systems with strong volume dependence of magnetic characteristics.

A number of the DFT studies of α -MnAs have been performed (see, e.g., Refs. 14 and 15). They agree in the main features of the density of states. Recently Niranjani *et al.*¹ reported the ultrasoft pseudopotential calculations of the β phase. By comparison of the total energies of the ferromagnetic and antiferromagnetic configurations they came to the conclusion that the β phase is characterized by the presence of antiferromagnetically ordered planes. The exchange interaction between planes is assumed to be very weak which leads to random relative orientations of the magnetic moments of different planes. Therefore the system as a whole does not possess a long-range magnetic order.

The long-term coexistence of apparently contradicting viewpoints on the magnetism of this important system makes crucial a systematic parameter-free microscopic study of the exchange interactions and magnetic transition temperatures in MnAs. Very recently Rungger and Sanvito² performed a detailed study of the magnetostructural properties of MnAs. Using pseudopotential SIESTA code¹⁶ they calculated the total energies of a number of collinear magnetic configurations for various crystal structures. The energies were fitted with a classical Heisenberg Hamiltonian. The exchange parameters obtained were employed to estimate the Curie temperature of the system. Rungger and Sanvito drew the conclusion that above T_1 the β phase is already in the paramagnetic state. The anomalous magnetic susceptibility between T_1 and T_2 is explained by the variation of the Curie temperature accompanying the continuous structural transformation.

In the given paper we use the frozen-magnon approach to calculate the exchange parameters and magnetic transition temperatures of the α and β phases. The magnetic transition temperatures are estimated and the nature of the β phase is discussed. The limits of the Heisenberg model are revealed. The unusual behavior of the induced As moments is obtained and related to the canting of the Mn moments.

II. CALCULATIONAL DETAILS

The NiAs and MnP crystal structures are presented in Fig. 1. The unit cells of the structures contain, correspondingly, two and four Mn atoms. In the NiAs structure, the Mn atoms form a simple hexagonal lattice with the primitive translation

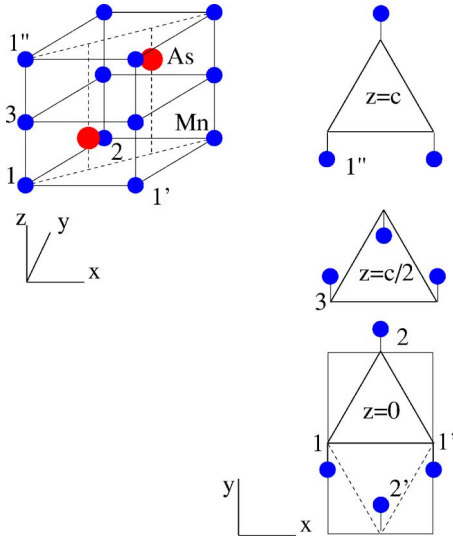


FIG. 1. (Color online) Left part: MnAs in NiAs-type structure. In the calculations we used the experimental parameters of the hexagonal lattice: $a=7.039$ a. u., $\frac{c}{a}=1.534$. Right part: A schematic presentation of the MnP-type structure. The shift of the Mn atoms for three horizontal levels is shown. The same numbering of atoms is used in both parts of the picture. The rectangle in the $z=0$ level shows the projection of the orthorhombic unit cell on the xy plane. Weak vertical shifts of the Mn atoms and the shifts of the As atoms are not shown. The coordinates of the Mn atoms are $(0, -\alpha, -\beta)$, $(\frac{1}{2}, \frac{1}{2} + \alpha, \beta)$, $(0, \alpha, \frac{1}{2} - \beta)$, $(\frac{1}{2}, \frac{1}{2} - \alpha, \frac{1}{2} + \beta)$ and the coordinates of the As atoms are $(\frac{1}{2}, \frac{1}{6} + \gamma, \frac{1}{4} + \delta)$, $(0, -\frac{1}{3} + \gamma, \frac{1}{4} - \delta)$, $(0, \frac{1}{3} - \gamma, \frac{3}{4} - \delta)$, $(\frac{1}{2}, -\frac{1}{6} - \gamma, \frac{3}{4} + \delta)$. Here the three Cartesian coordinates are given, respectively, in units of lattice parameters a , $b=\sqrt{3}a$, c . We used $\alpha=0.0271$, $\beta=0.0047$, $\gamma=0.0020$, $\delta=0.0245$ (Ref. 1). The parameter a of the MnP structure is obtained by the 1% contraction of the parameter a of the NiAs structure. The same c parameter is used.

along the z axis being half of the corresponding translation of the NiAs structure. Therefore the Mn subsystem taken separately has a higher periodicity than the system as a whole. In the MnP structure, the periodicity of the Mn positions coincides with the periodicity of the structure as a whole.

The calculations are performed with the augmented spherical waves (ASW) method.¹⁷ The exchange-correlation potential is chosen in the generalized gradient approximation.¹⁸

To estimate exchange interactions we map the system on the classical Heisenberg Hamiltonian

$$H_{eff} = - \sum_{\mu, \nu} \sum_{\mathbf{R}, \mathbf{R}'} J_{\mathbf{R}\mathbf{R}'}^{\mu\nu} \mathbf{e}_{\mathbf{R}}^{\mu} \mathbf{e}_{\mathbf{R}'}^{\nu} \quad (\mu\mathbf{R} \neq \nu\mathbf{R}') \quad (1)$$

In Eq. (1), the indices μ and ν number different sublattices and \mathbf{R} and \mathbf{R}' are the lattice vectors specifying the atoms within sublattices, $\mathbf{e}_{\mathbf{R}}^{\mu}$ is the unit vector pointing in the direction of the magnetic moment at site (μ, \mathbf{R}) .

The exchange parameters are evaluated using the frozen-magnon approach.¹⁹ The calculation of the exchange parameters of a multiple-sublattice system includes several steps and is more involved than in a single-sublattice case.²⁰ In

this paper, to simplify calculations we use the property of the NiAs structure that the cation atoms form a simple hexagonal lattice with higher periodicity than the structure as a whole. Since this cation lattice has one atom per unit cell the calculational scheme developed for single-sublattice systems can be applied. The energy of the spiral magnetic configurations (frozen magnons) of the form

$$\theta_{\mathbf{R}}^{\nu} = \theta, \quad \phi_{\mathbf{R}}^{\nu} = \mathbf{q} \cdot (\mathbf{R} + \boldsymbol{\tau}_{\nu}) \quad (2)$$

is calculated for the wave vectors \mathbf{q} varying within the Brillouin zone (BZ) corresponding to the Mn lattice that is twice the BZ of the NiAs structure. In Eq. (2), θ and ϕ are the polar and azimuthal angles and vector $\boldsymbol{\tau}_{\nu}$ determines the position of the atom of the ν th sublattice of the Mn atoms. In all calculations the direction of the induced As moments was kept parallel to the direction of the net magnetization (z axis).

In the calculations we used $\theta=30^{\circ}$. The magnetic-force theorem²² was employed in most of the calculations which allows us to estimate the energies of the nonequilibrium magnetic states avoiding self-consistent calculations. Within the Heisenberg model the energy of the frozen magnons takes the form

$$E(\theta, \mathbf{q}) = E_0(\theta) + \sin^2 \theta J(\mathbf{q}). \quad (3)$$

A uniform mesh of the frozen-magnon wave vectors over the first Brillouin zone has been employed. The interatomic exchange parameters are obtained by the Fourier transformation of $J(\mathbf{q})$. For the β phase the situation is more complex since the Mn sublattice is distorted and the extra periodicity characteristic for the α phase is lost. Since, however, the atomic displacements are rather small we apply the same procedure also for the β phase. In the calculations of the frozen magnons for the β phase the \mathbf{q} -mesh is slightly modified to take into account the contraction of the lattice.

III. CALCULATIONAL RESULTS

A. Density of states and magnetic moments

The densities of states (DOS) of the ferromagnetic MnAs in α and β phases are presented in Fig. 2. The calculated magnetic moments are $m_{\text{Mn}}=3.32\mu_B$ and $m_{\text{As}}=-0.10\mu_B$ for the α phase and $m_{\text{Mn}}=3.10\mu_B$ and $m_{\text{As}}=-0.40\mu_B$ for the β phase. The measured magnetic moment in the α phase is $m_{\text{MnAs}}=3.4\mu_B$ per chemical unit that is in good agreement with the calculated value. The DOS reveals strong hybridization of the Mn 3d and As 4p states. In the α phase the hybridized states form, for example, the spin-down feature with the center at about 0.15 Ry below the Fermi level. In the β phase the corresponding feature of the spin-down DOS becomes broader and moves closer to the Fermi level. The spin-up feature of the β -DOS at the Fermi level also contains hybridized states. The presence of highly hybridized states close to the Fermi level is an important property of the system.

To verify the existence of the low-spin state in the α phase, the fixed-spin-moment²¹ calculations have been performed for magnetic configurations with different angles be-

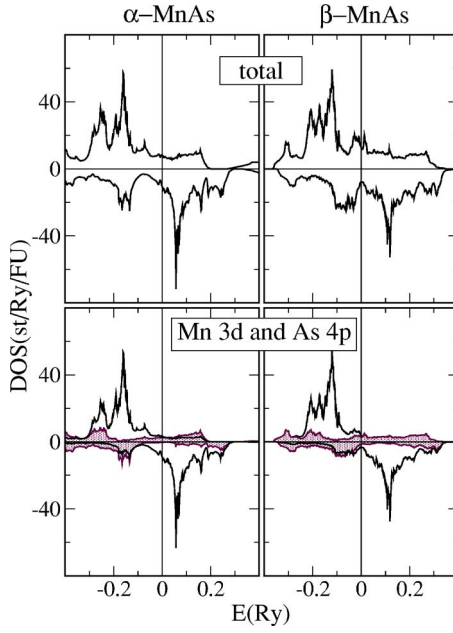


FIG. 2. (Color online) The spin-resolved DOS of α and β MnAs. In the lower panels the filled curves present As 4p DOS and the unfilled curves are Mn 3d DOS. The densities of states are given per chemical formula unit.

tween neighboring atomic moments. All calculations gave similar dependences of the energy on the value of the Mn moment. The functions have one minimum at m_{Mn} close to the ground-state value that excludes the existence of the low-spin state. The weak dependence of the atomic moment on the magnetic configuration shows that MnAs is an itinerant-electron material with well-defined atomic moments.

B. Exchange interactions and magnetic transition temperatures

The leading interatomic exchange interactions obtained on the basis of the frozen-magnon calculations are collected in Table I. There is a striking difference in the patterns of the exchange interactions of two phases. In the α phase the strongest is the ferromagnetic interaction between atoms 1

TABLE I. Calculated leading interatomic exchange parameters $J_{1\mu}$ and intersublattice exchange parameters $J_{1\mu}^0$ (in mRy) for α and β phases. The labeling of the atoms is according to Fig. 1. The exchange parameters $J_{\nu\mu}$ and $J_{\nu\mu}^0$ ($\nu \neq 1$) can be obtained from the parameters with $\nu=1$ taking into account the symmetry of the lattice.

	J_{12}	J_{13}	$J_{11'}$	$J_{11''}$	$J_{12'}$
α -MnAs	0.49	1.52	0.49	-0.37	0.49
β -MnAs	0.77	-0.57	0.57	0.44	0.79
		J_{11}^0	J_{12}^0	J_{13}^0	J_{14}^0
α -MnAs		0.87	2.39	2.87	0.63
β -MnAs		1.93	3.53	-1.80	0.93

and 3 of the neighboring hexagonal planes. In the β phase this interaction becomes antiferromagnetic. The interaction with the second nearest neighbor along the z axis also changes sign. The exchange interactions within the horizontal planes are ferromagnetic in both cases. However, also here there is large quantitative difference in the parameters. The ferromagnetic in-plane interaction is stronger in the β phase. The decreased symmetry of the β phase leads to a partial lifting of the degeneracy of the exchange parameters ($J_{11'}=J_{12'}=J_{12}$ in the α phase).

The big difference between the exchange interactions of the α and β phases can be related to the important difference in the DOS of the two phases (Fig. 2), in particular, in the region close to the Fermi energy. The change of the DOS is reflected in the strong variation of the induced As moment. The physical origin of these big changes lies in the sensitivity of the interatomic hybridization to the atomic shifts. This sensitivity is a characteristic feature of the hexagonal MnAs.

Note that the character of the changes in exchange parameters obtained in our calculations differs considerably from the results of the calculations by Rungger and Sanvito. It is, however, important to notice that in our calculations of the exchange parameters we used the energies of a large number of noncollinear magnetic configurations with the angles between neighboring magnetic moments distributed between zero and 2θ whereas Rungger and Sanvito used the energies of collinear configurations with the angles between atomic spins either zero or 180° . In systems where the exchange parameters are sensitive to the variations of the electronic structure these two schemes can give substantially different estimations. (In Ref. 2, the DOSs are not shown that would be useful for the comparison of two calculations.)

The value of the Curie temperature of a single-sublattice system is given within the mean-field approximation (MFA) and random-phase approximation (RPA) by the expressions

$$k_B T_C^{MFA} = \frac{2}{3} J(0), \quad \frac{1}{k_B T_C^{RPA}} = \frac{3}{2N} \sum_{\mathbf{q}} \frac{1}{J(\mathbf{0}) - J(\mathbf{q})}, \quad (4)$$

where $J(0) \equiv J_0$ is the sum of all Heisenberg exchange parameters connecting a given Mn atom with other Mn atoms.

The MFA values of the Curie temperature are 711 and 484 K correspondingly for the α and β phases. The RPA value for the α phase is 574 K. For the β phase, the energies of the frozen magnons for \mathbf{q} values close to $(0, 0, \frac{2\pi}{c})$ are weakly negative revealing the instability of the ferromagnetic state (see discussion below). Since the RPA expression for the Curie temperature contains reversed values of the magnon energies it becomes numerically unstable for the β phase. On the other hand, the MFA evaluates an average exchange field acting on each atom and still provides useful information.

The MFA value of the Curie temperature of the α phase is substantially higher than the experimental estimation of about 400 K obtained by the extrapolation of the magnetization curve of the α phase to the zero value. The RPA gives the Curie temperature closer to the experimental value though still overestimating it. We will come back to the rea-

sons for this overestimation later turning now to the discussion of antiferromagnetic configurations as possible ground states of the system.

To include the nonferromagnetic states into consideration we treat both α and β MnAs as four-sublattice systems with sublattices corresponding to the four atoms in the unit cell of the MnP structure (Fig. 1). Such a treatment allows us to account for the possibility of the antiparallel orientation of the atomic moments of different sublattices and to estimate the magnetic transition temperatures of the corresponding magnetic structures.

Within the MFA, the magnetic transition temperatures of different magnetic states of a multiple-sublattice system are given by the expression $k_B T_i^{MFA} = \frac{2}{3} \lambda_i$ where λ_i are the eigenvalues of the matrix of intersublattice exchange interactions,²³

$$J_{\nu\mu}^0 = \sum_{R_\beta} J_{[\nu 0][\mu R_\beta]}. \quad (5)$$

The eigenvector corresponding to λ_i determines the i th magnetic structure. The state with the largest λ_i is the magnetic ground state of the system.

Since all interatomic exchange parameters are known from previous calculations they can be used to evaluate the intersublattice exchange parameters $J_{\nu\mu}^0$ for $\nu, \mu=1, 2, 3, 4$ (Table I). In the α phase, all intersublattice parameters are ferromagnetic. Therefore the largest eigenvalue corresponds to the ferromagnetic configuration with $T_C=711$ K (this is exactly the value we obtained above in the consideration of the system as a single-sublattice ferromagnet). The next eigenvalue is much smaller ($\lambda_2=0.72$ mRy, $T_N=76$ K) and characterizes the magnetic transition temperature (Néel temperature) for structure $(+-+)$ consisting from the antiferromagnetic horizontal planes. In the notation $(+-+)$, + and - denote opposite directions of the moments of the corresponding sublattices $\mu=1, 2, 3, 4$.

In the β phase the interaction between the first and third sublattices is antiferromagnetic. As a result, the largest eigenvalue $\lambda_1=6.32$ mRy corresponds in this case to the antiferromagnetic structure $(++--)$ that constitutes the ground state of the Heisenberg system with the given set of the exchange parameters. The estimated value of the magnetic transition temperature is $T_N=625$ K. This antiferromagnetic structure is formed by the ferromagnetic horizontal planes that are oriented antiparallely with respect to each other. The eigenvalue corresponding to the ferromagnetic state $\lambda_2=4.60$ mRy is second in the value and gives the estimation of $T_C=484$ K that is exactly the value of the Curie temperature obtained above in the treatment where the ferromagnetic state only was considered.

C. Limits of the Heisenberg model

Before discussing further the phase transitions in MnAs we address an important question of the applicability of the Heisenberg model to the quantitative description of MnAs. The exchange parameters used in the estimations were evaluated for the ferromagnetic reference state. In an ideal Heisenberg system the parameters do not depend on the reference

state. Our studies are, however, based on the first-principles DFT calculations for an itinerant electron system. Therefore the sensitivity to the procedure of the evaluation of the Heisenberg parameters must be verified.

For the β MnAs, the use of the exchange parameters calculated for the ferromagnetic reference state resulted in the prediction of an antiferromagnetic ground state. To verify this prediction, a direct DFT calculation of this antiferromagnetic state has been performed. In disagreement with the prediction, the energy of the antiferromagnetic configuration was obtained to be higher than the energy of the ferromagnetic configuration by 12 mRy per Mn atom. Therefore despite well-defined moments of Mn atoms, the Heisenberg model has limited quantitative validity in MnAs. The overestimation of the magnetic transition temperatures is another factor supporting this conclusion. It is beyond the scope of this paper to apply more complex model Hamiltonians to the parameter-free studies of the thermodynamics of MnAs. The number of such studies for magnetic compounds with well defined atomic moments is still very small (see Refs. 24–26 for the examples of exceptions). The importance of the problem, on the one hand, and increased computer power, on the other hand, will certainly make the development and application of new approaches to the thermodynamics of itinerant-electron systems an important task for the nearest future researches.

To get a guideline for the direction of necessary improvements, the physical reason for the limits of the Heisenberg model in the case of MnAs must be understood. The following consideration helps to shed light on this problem.

Let us consider two groups of atoms with the magnetic moments deviating from the z axis by polar angle θ . E_2 is the energy of the configuration where the sublattices numbered by ξ have azimuthal angle $\phi=0$ and the sublattices numbered by χ have azimuthal angle $\phi=180^\circ$. E_1 is the energy of the configuration where both groups of atoms have $\phi=0$. Then within the Heisenberg model, it can be shown that

$$\Delta E(\theta) = E_2(\theta) - E_1(\theta) = 4 \sin^2 \theta \sum_{\xi\chi} J_{\xi\chi}^0. \quad (6)$$

The calculations (Fig. 3) have been performed for $\xi=1, 2$ and $\chi=3, 4$, first, with the use of the force theorem and, second, by achieving self-consistency for all magnetic configurations. In both cases, $\Delta E(\theta)$ deviates from the simple Heisenberg form [Eq. (6)]. Remarkable, however, is that the results of two types of calculations differ substantially. In the self-consistent calculations, the minimum of the total energy is shifted from $\theta=0$ to $\theta \sim 10^\circ$. Therefore the ground state of the α MnAs appears to be a slightly canted ferromagnet. The range of the energy variation of the $\Delta E(\theta)$ curve obtained in the self-consistent calculations is smaller than in the force-theorem calculations. Therefore the exchange parameters evaluated with the force theorem are overestimated in this case that explains the overestimation of the Curie temperature obtained above.

An important reason for both the non-Heisenberg behavior and the overestimation of the Curie temperature we find in the behavior of the induced As moment. Since the states of As mediate exchange interaction between the Mn moments

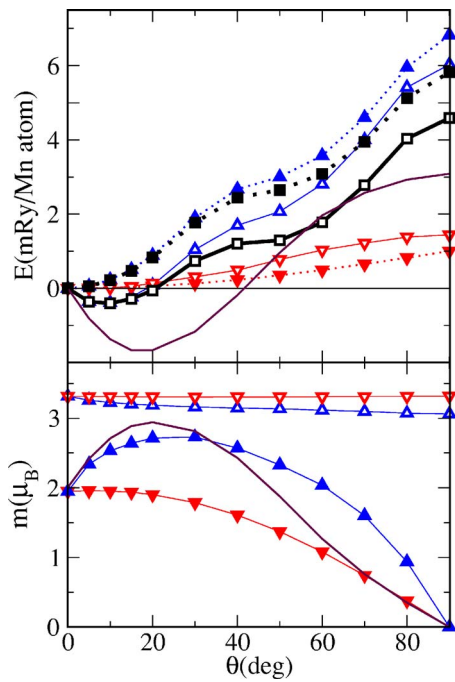


FIG. 3. (Color online) The θ dependence of the total energy (upper panel) and magnetic moments (lower panel). In the upper panel the broken curves with filled symbols present the results of force-theorem calculations for the α MnAs. The solid curves with unfilled symbols show corresponding results of self-consistent calculations. In both cases, the down triangles present the E_1 values and the up triangles present the E_2 values. The squares give the difference $\Delta E = E_2 - E_1$. The solid curve without symbols presents E_2 for the β MnAs (for better visual comprehension the curve is scaled with factor 0.5). All energies are counted from the energy of the ferromagnetic state ($\theta = 0$). In the lower panel the curves with symbols present the self-consistent moments in the α phase. The unfilled symbols give the values of the Mn moment (up triangle for the E_1 case and down triangle for the E_2 case). The filled symbols give the corresponding values of the induced As moments (these curves are scaled with factor -20). The curve without symbols presents the induced As moments of the β phase (scaled with factor -5).

the properties of these states, in particular the value of the induced As moment, are of primary importance. From the symmetry reasons, the induced As moment at $\theta = 90^\circ$ is zero. The calculated induced As moment in the θ interval from 0 to 90° deviates strongly from a simple proportionality to the net magnetic moment of the Mn subsystem. Surprisingly, the induced moment first increases with increasing θ making the dependence $m_{\text{As}}(\theta)$ nonmonotonous.

The nonmonotonous character of the dependence reflects the particular properties of the electronic structure of the system. The following consideration helps us to understand the physical reason for such a behavior. With the deviation of the Mn moments from the parallel directions the spin projection of all electron states of the system ceases to be a good quantum number. The As $4p$ states can now couple simultaneously to both Mn $3d$ spin-up and Mn $3d$ spin-down states (Fig. 4). Depending on the deviation angle, different regimes should be considered. For small θ , a weak coupling of the

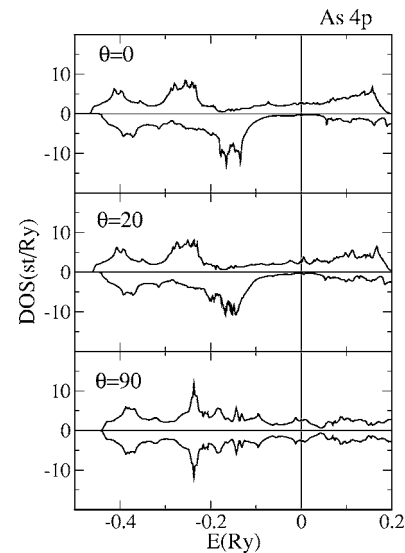


FIG. 4. The spin-resolved As $4p$ DOS for three magnetic configurations in the α phase.

As $4p$ states to the Mn $3d$ states with opposite spin projection modifies the As $4p$ spin-up and spin-down DOS only slightly. The comparison of the DOS for $\theta = 0$ and $\theta = 20^\circ$ shows that an important role is played by the coupling of the As $4p$ spin-down states to the Mn $3d$ spin-up states at about 0.2 Ry below the Fermi energy. As a result, the number of the occupied spin-down As $4p$ states increases. Since the induced As moments are opposite to the Mn magnetization, the value of the As moment increases (despite decreasing net Mn magnetization).

For large θ , the couplings to both spin components of the Mn $3d$ states become close to each other leading, within the self-consistent procedure, to strongly decreasing induced moment. Since the As states mediate the exchange interaction between Mn atoms this peculiar behavior of the induced As moment is important for the Mn-Mn exchange interaction: the θ dependence of the exchange parameters and therefore non-Heisenberg behavior of the system can be expected. We relate a weak canting of the magnetic structure obtained in the total-energy calculations (Fig. 3) to the increase of the induced moment of the As atoms for small nonzero θ . The mechanism of the formation of a noncollinear magnetic structure through the nonmonotonous behavior of the induced moments of the atoms mediating exchange interaction has not yet been discussed in the literature and must receive an adequate attention in the future. The comparison of the results of the calculations based on the force theorem with the results obtained self-consistently shows that the force theorem calculations underestimate the effects related to the variation of the induced moments.

The deviation from the Heisenberg model is even stronger in the case of the β phase. Again we relate this property to the dependence of the induced As moment on the configuration of the Mn moments. Since in the β phase the induced moment is larger than in the α phase, the effect is stronger. The predicted ground state is here again a canted ferromagnetic configuration with the canting angle of about 20° .

IV. CONCLUSIONS

The results of the calculations suggest the following interpretation of the magnetic properties of MnAs that in the main points agrees with the conclusions by Rungger and Sanvito. Since the MFA estimations of magnetic critical temperatures for the β phase are considerably lower than the estimated T_C of the α phase we draw the conclusion that at the temperature T_1 of the α - β transition the β phase is already in the paramagnetic state. The anomalous behavior of the magnetic susceptibility between T_1 and T_2 can be explained by the variation of both the atomic moments and the exchange interactions accompanying the continuous variation of the atomic structure in this temperature interval. Indeed, our calculations have shown that the magnetic moments and, especially, the exchange interactions depend on the atomic configuration. Since the Curie-Weiss law is characteristic for the systems with temperature-independent

atomic moments and exchange parameters, it does not apply here. Above T_2 the atomic structure stabilizes leading to the Curie-Weiss behavior of the paramagnetic susceptibility.

Summarizing, we performed parameter-free evaluation of the exchange parameters and critical temperatures of α and β MnAs that suggest that at the point of the α - β phase transition the β phase is already in the paramagnetic state. The abnormal temperature behavior of the magnetic susceptibility of the β phase is explained by the strong dependence of the exchange parameters on the atomic structure that experience continuous variation in the β phase. We found that the system, despite well-defined Mn moments, cannot be quantitatively described within the Heisenberg model. We relate this property to the properties of induced As moments. We found unusual nonmonotonous behavior of the induced As moments and have shown that such a behavior can be the reason for the canting of the atomic Mn moments.

-
- ¹M. K. Niranjan, B. R. Sahu, and L. Kleinman, *Phys. Rev. B* **70**, 180406 (2004).
- ²I. Rungger and S. Sanvito, *Phys. Rev. B* **74**, 024429 (2006).
- ³J. Mira, F. Rivadulla, J. Rivas, A. Fondado, T. Guidi, R. Caciuffo, F. Carsughi, P. G. Radaelli, and J. B. Goodenough, *Phys. Rev. Lett.* **90**, 097203 (2003).
- ⁴H. Wada and Y. Tanabe, *Appl. Phys. Lett.* **79**, 3302 (2001).
- ⁵A. K. Das, C. Pampuch, A. Ney, T. Hesjedal, L. Däweritz, R. Koch, and K. H. Ploog, *Phys. Rev. Lett.* **91**, 087203 (2003).
- ⁶H. Yamaguchi, A. K. Das, A. Ney, T. Hesjedal, C. Pampuch, D. M. Schaadt, and R. Koch, *Europhys. Lett.* **72**, 479 (2005).
- ⁷F. Iikawa, M. J. S. P. Brasil, C. Adriano, O. D. D. Couto, C. Giles, P. V. Santos, L. Däweritz, I. Rungger, and S. Sanvito, *Phys. Rev. Lett.* **95**, 077203 (2005).
- ⁸C. P. Bean and D. S. Rodbell, *Phys. Rev.* **126**, 104 (1962).
- ⁹C. Guillaud, *J. Phys. Radium* **12**, 223 (1951).
- ¹⁰R. H. Wilson and J. S. Kasper, *Acta Crystallogr.* **17**, 95 (1964).
- ¹¹G. E. Bacon and R. Street, *Nature (London)* **175**, 518 (1955).
- ¹²C. Kittel, *Phys. Rev.* **120**, 335 (1960).
- ¹³J. B. Goodenough and J. A. Kafalas, *Phys. Rev.* **157**, 389 (1967).
- ¹⁴L. M. Sandratskii, R. F. Egorov, and A. A. Berdyshev, *Phys. Status Solidi B* **103**, 511 (1981).
- ¹⁵Y.-J. Zhao, W. T. Geng, A. J. Freeman, and B. Delley, *Phys. Rev. B* **65**, 113202 (2002).
- ¹⁶J. M. Soler, E. Artacho, J. D. Gale, A. Garcia, J. Junquera, P. Ordejon, and D. Sanchez-Portal, *J. Phys.: Condens. Matter* **14**, 2745 (2002).
- ¹⁷A. R. Williams, J. Kübler, and C. D. Gelatt, *Phys. Rev. B* **19**, 6094 (1979).
- ¹⁸J. P. Perdew and Y. Wang, *Phys. Rev. B* **45**, 13244 (1992).
- ¹⁹L. M. Sandratskii and P. Bruno, *Phys. Rev. B* **67**, 214402 (2003).
- ²⁰E. Sasioglu, L. M. Sandratskii, and P. Bruno, *Phys. Rev. B* **70**, 024427 (2004).
- ²¹K. Schwarz and P. Mohn, *J. Phys. F: Met. Phys.* **14**, L129 (1984).
- ²²A. I. Liechtenstein, M. I. Katsnelson, V. P. Antropov, and V. A. Gubanov, *J. Magn. Magn. Mater.* **67**, 65 (1987).
- ²³P. W. Anderson, in *Solid State Physics*, edited by F. Seitz and D. Turnbull (Academic, New York, 1963), Vol. 14, pp. 99–214.
- ²⁴J. Kübler, *Theory of Itinerant Electron Magnetism* (Clarendon, Oxford, 2000).
- ²⁵R. Y. Gu and V. P. Antropov, *Phys. Rev. B* **72**, 012403 (2005).
- ²⁶M. Ležaić, Ph. Mavropoulos, J. Enkovaara, G. Bihlmayer, and S. Blügel, *Phys. Rev. Lett.* **97**, 026404 (2006).